Journal of Comparative Physiology B
https://doi.org/10.1007/s00360-022-01458-1

ORIGINAL PAPER

How the green crab *Carcinus maenas* copes physiologically with a range of salinities

Giorgi Dal Pont[1,2,3] · Beverly Po[1,2] · Jun Wang[1,2,4] · Chris M. Wood[1,2]

Received: 20 July 2022 / Revised: 7 August 2022 / Accepted: 18 August 2022

Abstract

To evaluate the physiological ability to adjust to environmental variations of salinity, *Carcinus maenas* were maintained in 10, 20, 32 (control), 40, and 50 ppt (13.8 ± 0.6 °C) for 7 days. Closed respirometry systems were used to evaluate oxygen consumption ($\dot{M}O_2$), ammonia excretion (Jamm), urea-N excretion (Jurea-N) and diffusive water fluxes (with ^3H_2O). Ions, osmolality, metabolites, and acid–base status were determined in the hemolymph and seawater, and transepithelial potential (TEP) was measured. At the lowest salinity, there were marked increases in $\dot{M}O_2$ and Jamm, greater reliance on N-containing fuels to support aerobic metabolism, and a state of internal metabolic alkalosis (increased [HCO_3^-]) despite lower seawater pH. At higher salinities, an activation of anaerobic metabolism and a state of metabolic acidosis (decreased [HCO_3^-] and increased [lactate]), in combination with respiratory compensation (decreased PCO_2), were detected. TEP became more negative with decreasing salinity. Osmoregulation and osmoconformation occurred at low and high salinities, respectively, with complex patterns in individual ions; hemolymph [Mg^{2+}] was particularly well regulated at levels well below the external seawater at all salinities. Diffusive water flux rates increased at higher salinities. Our results show that *C. maenas* exhibits wide plasticity of physiological responses when acclimated to different salinities and tolerates substantial disturbances of physiological parameters, illustrating that this species is well adapted to invade and survive in diverse habitats.

Keywords Ionoregulation · Nitrogen metabolism · Diffusive water exchange · Acid–base regulation · Transepithelial potential

Introduction

One characteristic of the green crab *Carcinus maenas* that has contributed to its worldwide success as an exotic invader is its remarkable euryhalinity (Behrens-Yamada 2001; Klassen and Locke 2007; Leignel et al. 2014). Adults are reported to tolerate a range of salinities between < 5 and > 50 ppt (Bateman 1933; Zanders 1980; Siebers et al. 1982; Spaargaren 1982; McGaw 1991; McGaw et al. 1999) for periods varying from days to weeks. There have been many physiological studies on the mechanisms involved, most of them focusing on the effects of reduced salinity rather than elevated salinity. In general, *C. maenas* osmoregulates below about 26 ppt, employing active mechanisms to keep hemolymph osmolality above that of the external seawater. Above 26 ppt, it osmoconforms to the external seawater, though individual ions are still regulated (reviewed by Henry et al. 2012).

Landmark studies of salinity effects on *C. maenas* include those of Webb (1940) who highlighted the

Communicated by B. Pelster.

✉ Chris M. Wood
woodcm@zoology.ubc.ca

Giorgi Dal Pont
giorgidalpont@gmail.com

Beverly Po
pobev@zoology.ubc.ca

Jun Wang
wangjun@ouc.edu.cn

[1] Department of Zoology, The University of British Columbia, Vancouver, BC V6T 1Z4, Canada

[2] Bamfield Marine Sciences Centre, Bamfield, BC V0R 1B0, Canada

[3] Integrated Group for Aquaculture and Environmental Studies, Department of Animal Science, Federal University of Paraná, Curitiba, Paraná 83035-050, Brazil

[4] College of Marine Life Sciences, Ocean University of China, Qingdao 266003, China

Published online: 30 August 2022

regulation of hemolymph ions at low salinity and suggested that active uptake must be involved. This idea was confirmed by later workers (Shaw 1961; Siebers et al. 1982; Henry et al. 2002, 2003), who provided evidence for the key involvement of the posterior gills, which are enriched in Na^+ K^+ ATPase and carbonic anhydrase, especially when salinity is reduced. The activity of Na^+ K^+ ATPase contributes to the negative transepithelial potential (TEP, inside relative to outside as 0 mV) across the posterior gills that becomes progressively more negative as salinity is lowered (Siebers et al. 1986). However, this trend has not been detected in the TEP of the whole animal (Greenaway 1976; Zanders 1980; Winkler 1986). Other key findings include persistent increases in the rates of whole organism O_2 consumption ($\dot{M}O_2$) (Siebers et al. 1972; Taylor 1977) and ammonia excretion (Jamm) (Spaargaren 1982) when crabs are transferred to low salinities. The latter may involve an active transport process for ammonia, powered by Na^+ and K^+ ATPase and linked in some way to Na^+ uptake (Weihrauch et al. 1999, 2017). A metabolic alkalosis (increased pH and HCO_3^- with more or less unchanged PCO_2) also develops in the hemolymph of crabs transferred to lower salinities (Zanders 1980; Truchot 1973, 1981). The influence of salinity on the apparent water permeability, as measured by the diffusive flux of radiolabeled water, has been examined by many investigators [reviewed by Rasmussen and Andersen (1996)], but there are discrepancies in the conclusions. Most authors have reported that diffusive water flux rates decline slightly with decreases in salinity (Smith 1970; Rainbow and Black 2001; Berlind and Kamemoto 1977; Rasmussen and Bjerregaard 1995), but Rudy (1967) reported no detectable changes.

In most of the salinity studies cited above, only one or two of the major physiological parameters were measured, and often only under control conditions (30–35 ppt) versus markedly reduced salinity, so thresholds were not defined. Relatively few studies have looked at hypersaline conditions (above 35 ppt). Against this background, our principal objective was to measure a wide range of parameters at the whole organism level in a single batch of crabs acclimated to salinities of 10 ppt, 20 ppt, 32 ppt (32 ppt = 100% SW), 40, and 50 ppt. These parameters included oxygen consumption, ammonia excretion, urea-N excretion, hemolymph concentrations of ammonia, urea-N, total protein, total amino acids, glucose, lactate, major ions (Na^+, K^+, Ca^{2+}, Mg^{2+}, Cl^-) and osmolality, hemolymph acid–base status (pH, [HCO_3^-], PCO_2), TEP of the whole crab, as well as diffusive exchange rates of water and internal exchangeable water pools using ^3H_2O. These measurements were made with the goal of understanding the interrelationships of various responses, as well as the physiological parameters that may limit tolerance to extreme salinities in this highly successful invasive species.

Materials and methods

Animal collection and acclimation

Male green crab (*C. maenas*; $n = 140$; weight = 90.8 ± 3.5 g) were captured using wire crab traps baited with fish fillets in the estuarine area near Seddall Island, Ecoole, Regional District of Alberni-Clayoquot, British Columbia, Canada (49° 05′ 00.0″ N 125° 10′ 21.6″ W). At the laboratory, crabs were held for 1 week in 500-L tanks in a flow-through system filled with aerated seawater (12–14 °C, 32 ppt) and were fed ad libitum with fish fillets. Only crabs with carapace colored in different shades of green (and not red) were used.

Experimental design

Crabs were acclimated to different non-lethal water salinities [10, 20, 32 (control), 40 and 50 ppt] for 7 days. In a preliminary study we also exposed crabs to 5 and 60 ppt. However, at those salinities some mortalities (15–25%) were observed. As our goal was to study mechanisms of adjustment, rather than absolute salinity tolerance, experiments were restricted to the 10–50 ppt range. Lower salinities were obtained by diluting seawater with dechlorinated BMSC tap freshwater, which is very low in ions (Na^+ 0.300, Cl^- 0.233, K^+ 0.005, Ca^{2+} 0.144, Mg^{2+} 0.048 mmol L^{-1}). For the control salinity (32 ppt), we used plain filtered seawater. The salinity of the 32 ppt seawater was raised to 40 and 50 ppt using Instant Ocean™ salts (Spectrum Brands, Blacksburg, VA, USA). Water salinity was monitored using a portable conductivity meter (Cond 3110, WTW, Weilheim, Germany). Crabs were kept in groups of 12 animals at the salinities described above in static systems (50-L plastic tubs), with air flow supply (PO_2 ~ 80% saturation), maintained at the control temperature (13–14 °C). During this acclimation period, water was renewed (80%) daily and crabs were fasted.

Experimental series 1: effects of acclimation to different salinities on metabolic, ionoregulatory, and acid–base parameters

Experiments were conducted in glass containers (700 mL) covered with a dark plastic film to isolate crabs from outside visual stimuli, using a dark plastic mesh as a lid and fitted with tubing for constant air supply. To maintain the acclimation temperature, the containers were placed in a flow-through water bath. Prior to experimentation, crabs ($N = 8$ per salinity) were weighed and then placed in their individual containers for 12-h overnight settling at their acclimation

salinity (10, 20, 32, 40, or 50 ppt). Then, 100% of the SW was renewed with minimal disturbance. After 1 h, 90% of the SW volume was again renewed in the same way. Clean seawater at exactly the same salinity as the specific treatment was used in both water change procedures. Water samples (5 mL) were collected at 0, 1, 2, 3, and 4 h, for determination of the fluxes of total ammonia ($NH_4 + NH_3$) and urea-N.

Immediately after the end of the 4-h flux measurement, 90% of the water volume was replaced with air-saturated water for measurement of the oxygen consumption rate ($\dot{M}O_2$). The initial oxygen partial pressure (PO_2) was measured using a polarographic dissolved oxygen meter (Accumet AP84A, Fisher Scientific, Toronto, ON, Canada). The initial average (mean ± SEM) PO_2 was 155.0 ± 0.5 Torr. To avoid diffusion of O_2 from the atmospheric air to the water, the container lid was sealed with rubber latex (127 mm × 127 mm—Hygenic dental dam, Performance Health, Akron, OH, USA). Crabs were kept in this condition for 30 min and then a final PO_2 measurement was performed. Tests with blank chambers demonstrated that there was no detectable O_2 consumption, or production/loss of ammonia or urea-N under the conditions of the measurements.

Shortly after the end of the respirometry measurements, a water sample (20 mL) was taken from each container, and a venous hemolymph sample (500 µL) was drawn from the crab. The sample was taken from the arthrodial membrane sinus of the last walking leg, using a gas-tight glass syringe (Hamilton, Reno, NV, USA). The animals remained submerged during sampling. Water was analyzed for pH, ions (Na^+, K^+, Ca^{2+}, Mg^{2+}, Cl^-) and osmolality, and hemolymph was analyzed for acid–base status (pH, total $[CO_2]$), glucose, lactate, total ammonia, urea-N, ions and osmolality. Water pH, and hemolymph pH and total $[CO_2]$ were measured immediately. The remainder of the hemolymph sample was divided into several aliquots, immediately frozen in liquid nitrogen, and then stored at − 80 °C until analysis. Water samples were frozen at − 20 °C for later analysis.

Experimental series 2: effects of acclimation to different salinities on transepithelial potential (TEP)

Crabs ($N = 8$ per salinity) were surgically prepared the day before measurements of TEP. The crabs were cold anesthetized by packing in ice for 3–5 min and weighed. They were then immobilized using a home-made apparatus (wooden restraint board and rubber bands). A small hole was drilled through the dorsal carapace using a Dremel tool fitted with a dental drill bit (Dremel, Mount Prospect, II, USA). The hole was sized so as to snugly accommodate the TEP electrode (see below), and was located at the anterior margin of the pericardium, close to the ophthalmic artery. Double layers of latex dental dam (the same as used for respirometry) were then glued over the cleaned and dried top of the hole with cyanoacrylate glue (Krazy Glue, Westerville, OH, USA). A number was placed on dental dam for later identification of the crab. Crabs were returned to their group acclimation tanks (10, 20, 32, 40 and 50 ppt) for 12-h overnight recovery. On the next day, crabs were transferred into fresh solutions of the same salinities to which they had been acclimated for the measurement of TEP. The same surgery was used by Zimmer and Wood (2017) and no changes in behavior were observed.

Experimental series 3: effects of acclimation to different salinities on diffusive water fluxes

To measure the unidirectional diffusive water flux, acclimated crabs from each salinity ($N = 8$–14 per treatment) were individually placed in plastic containers coated with black film and filled with 0.5 L of the correct salinity to which 10 µCi of ^3H_2O (Perkin Elmer, Woodbridge, ON, Canada) had been added. Each container was placed in a water bath at the experimental temperature and continuously aerated for a 12-h overnight ^3H_2O loading period. Preliminary experiments demonstrated that this was more than sufficient to achieve diffusive equilibration with the internal water pool of the crab. Duplicate 4-mL water samples were taken at the end of the equilibration period. Then, crabs were rinsed in radioisotope-free acclimation water for 1 min, and transferred to aerated experimental containers filled with 1 L of radioisotope-free seawater at the acclimation salinity (10, 20, 32, 40, or 50 ppt). Four mL of water was sampled at the beginning (time 0) and at 5, 10, 15, 20, 25, 30, 40, 50, 60, 75, and 90 min, with final duplicate 4-mL samples taken at approximately 12 h when diffusive equilibration (washout) was again complete. Eight mL of Ultima Gold AB fluor (Perkin-Elmer, Wellesley, MA, USA) was added to the 4-mL water sample (2:1 ratio). After 12-h resting in the dark to minimize chemiluminescence, the concentration of ^3H_2O in the samples was determined using a liquid scintillation counter (LS6500, Beckman Coulter, Fullerton, CA, USA). Tests showed that quenching was constant within a salinity, so no corrections were made.

Analytical methods

Metabolite assays

The concentration of ammonia in the water was determined colorimetrically (595 nm) according to the method described by Verdouw et al. (1978). Hemolymph total ammonia (µmol $NH_4 + NH_3$ L^{-1}) was measured on freshly thawed samples using an enzymatic commercial assay kit (Raichem, Cliniqa, San Marcos, CA, USA), read at 340 nm. Crab hemolymph was used as a background matrix to correct the ammonia

standard curve (Giacomin et al. 2019b), and the same standard stock was used as for the water ammonia assay. Water and hemolymph urea-N concentrations (i.e., μmol-N L^{-1}, to account for the 2 nitrogens in urea) were determined through the colorimetric assay (525 nm) of Rahmatullah and Boyde (1980). Hemolymph glucose was determined at 340 nm using the Infinity™ Glucose Hexokinase Liquid Stable Reagent kit (Thermo Fisher, Middletown, VA, USA). Hemolymph lactate was measured at 340 nm using a modified version of the protocol described by Healy and Schulte (2012) and detailed by Dal Pont et al. (2019). The total concentration of hemolymph protein was determined at 595 nm by the colorimetric assay of Bradford (1976) using bovine serum albumin as a standard. A modified method of the ninhydrin assay of Moore and Stein (1954) was used to measure total amino acids in hemolymph. Prior to assay, hemolymph samples were deproteinized (1:4 ratio of 80% ethanol and hemolymph, gently mixed, then centrifuged for 60 s). In a test tube, 20 μL of the deproteinized sample and 300 μL of ninhydrin reagent (0.2% ninhydrin solution; Sigma-Aldrich, St. Louis, MO, USA) were mixed and placed in boiling water (100 °C) for 20 min. Once cold, 1.6 mL of 50% n-propanol solution was added, followed by thorough vortexing. After standing for 10 min, the samples and a standard curve (0–10 mmol L^{-1} L-alanine solution) were read at 570 nm. All colorimetric and enzymatic assays were read on a SpectraMax 340PC plate reader (Molecular Devices, San Jose, CA, USA).

Acid–base measurements

Water and hemolymph samples were promptly measured for pH, in a water bath thermostatted to the acclimation temperature, using an MI-4156 Micro-Combination pH probe (Microelectrodes Inc., Bedford, NW, USA) and Accumet pH meter (Fisher Scientific, Toronto, ON, Canada), calibrated with Radiometer precision buffers (Radiometer-Copenhagen, Denmark). The total [CO_2] in the hemolymph was measured using a total CO_2 analyzer (Corning 965 CO_2 analyzer, Ciba Corning Diagnostic, Halstead, Essex, UK). PCO_2 and [HCO_3^-] were calculated as described below.

Ion and osmolality measurements

Hemolymph and water samples from the same crab were analyzed as matching pairs. A Wescor vapor pressure osmometer and Opti-Mole standards (Wescor 5100C, Logan, UT, USA) and a coulometric chloridometer (CMT10, Radiometer Copenhagen) were used to quantify osmolality (mOsm kg^{-1}) and chloride concentration (mmol L^{-1}), respectively, on water and hemolymph samples. A Varian AA240FS atomic absorption spectrophotometer (AAS) (Varian Medical Systems, Palo Alto, CA, USA), operated in flame mode with acetylene as the purging gas, was used to determine the concentrations (mmol L^{-1}) of Na^+, K^+, Ca^{2+} and Mg^{2+} in water and hemolymph samples. Prior to analyses, samples were diluted [$Na^+ = 100{,}000\times$ and $K^+ = 1500\times$ with distilled water and, $Ca^{2+} = 2000\times$ and $Mg^{2+} = 2000\times$ with 1% lanthanum chloride ($LaCl_3$) solution]. Standard curves based on linear absorbance versus concentration relationships were built for each ion. Commercially manufactured standard solutions (Fisher Scientific, Toronto, Canada) were read between every 15 experimental samples to ensure quality control.

Transepithelial potential measurements

The TEP (mV) was measured using 3 M KCl–agar bridges (PE 90 tubing; Becton, Dickinson and Co., Franklin Lakes, NJ, USA) connected via Ag/AgCl electrodes (World Precision Instruments, Sarasota, FL, USA) to a high-impedance voltmeter (pHM 82, Radiometer-Copenhagen). The measurement bridge was inserted through a pinhole in the dental dam into the hole drilled on the carapace. The entry point would seal itself when the measurement bridge was withdrawn. At the same time, the reference bridge was placed in the solution of the same chamber (10, 20, 32, 40, or 50 ppt). TEP measurements were made in quadruplicate with correction for the junction potential each time.

Calculations

The concentrations of ammonia-N and urea-N in the water were used to calculate net flux rates [Jamm {μmol-N $kg\ h^{-1}$} and Jurea-N (μmol-N $kg\ h^{-1}$)], respectively) using the following equations:

$$\text{Jamm} = \left[\left(\text{amm}_i - \text{amm}_f\right) \times V\right]/(W \times T), \tag{1}$$

$$\text{Jurea - N} = \left[\left(\text{urea - N}_i - \text{urea - N}_f\right) \times V\right]/(W \times T), \tag{2}$$

where amm_i and amm_f (μmol L^{-1}) and urea-N_i and urea-N_f (μmol urea-N L^{-1}; note two Ns per urea molecule) are, respectively, the initial and final ammonia and urea-N concentrations in the experimental solution during the flux period; V is the experimental water volume (L); W is the weight of the animal (kg); and T is the duration of the flux period (h).

To calculate the oxygen consumption rate ($\dot{M}O_2$, μmol O_2 $kg^{-1}\ h^{-1}$), PO_2 (%) values were first converted to PO_2 (Torr) considering the saturation vapor pressure at the specific water temperature, and then the following equation was applied:

$$\dot{M}O_2 = \left[\left(\left(PO_{2i} - PO_{2f}\right) \times \alpha O_2\right) \times V\right]/(W \times T), \tag{3}$$

where PO_{2i} and PO_{2f} represent the oxygen pressure in the water (Torr) at the start and end of the experiment,

respectively, αO_2 represents the oxygen solubility coefficient at each water salinity (Boutilier et al. 1984), and the other variables (V, W and T) are as described for Eqs. (1) and (2).

Measurements of Jamm, Jurea-N, and $\dot{M}O_2$ were used to calculate the nitrogen quotient (NQ):

$$NQ = \dot{M}_N/\dot{M}O_2, \tag{4}$$

where $\dot{M}_N$ is the sum of the excretion rates of the nitrogen compounds (Jamm and Jurea-N, μmol-N kg^{-1} h^{-1}).

Constants for pK and ammonia solubility at the appropriate temperature and ionic strength from Cameron and Heisler (1983) were used to calculate the fractionation of total ammonia (T_{Amm}) in hemolymph using the following equations:

$$\left[NH_3\right] = \frac{T_{Amm} \times \text{ antilog } (pH-pK)}{1 + \text{antilog } (pH - pK)}, \tag{5}$$

$$\left[NH_4^+\right] = T_{Amm} - \left[NH_3\right], \tag{6}$$

$$PNH_3 = \left[NH_3\right]/\alpha NH_3. \tag{7}$$

Equation (8) (McDonald et al. 1980) was used to calculate ΔH_m^+, the accumulation of metabolic (i.e., of non-respiratory origin) acidic equivalents (positive values), or basic equivalents (negative values) appearing in the hemolymph, relative to the mean acid–base status at 32 ppt (control):

$$\Delta H_m^+ = \left[HCO_3^-\right]_c - \left[HCO_3^-\right]_s - \beta \times \left(pH_c - pH_s\right), \tag{8}$$

where the subscripts "c" and "s" refer to the "control" and "sample" values of hemolymph [HCO_3^-] and pH, and β is the slope of the non-bicarbonate buffer (NBB) line for *C. maenas*. Truchot (1976b) reported that β was a linear function of total protein concentration in the hemolymph. As this did not change significantly across salinities in the present study, the mean β from the regression relationship of Truchot (1976b) was used. Data are expressed as mmol L^{-1}.

Hemolymph PCO_2 (Torr) was calculated using a rearrangement of the Henderson–Hasselbach equation:

$$PCO_2 = TCO_2/\left[\alpha CO_2 \times \left(1 + \text{antilog } \left(pH - pK_{app}\right)\right)\right], \tag{9}$$

where TCO_2 and pH are the total carbon dioxide concentration and pH measured in the hemolymph, respectively. αCO_2 is the solubility coefficient of carbon dioxide, and pK_{app} is the apparent carbonic acid dissociation constant in the hemolymph of *C. maenas* [tabulated by Truchot (1976a) for the appropriate acclimation salinity and temperature].

The concentration of [HCO_3^-] (mmol L^{-1}) in the hemolymph was calculated according to the following equation:

$$\left[HCO_3^-\right] = TCO_2 - (\alpha CO_2 \times PCO_2). \tag{10}$$

Diffusive water flux calculations followed closely those outlined by Giacomin et al. (2019a) and were based on the total amount of radioactivity (cpm) taken up by each individual crab during the ^3H_2O loading period (R_{Total}). This was calculated from the total amount of radioactivity in the experimental container (crab + water) at the end of the washout period, plus all radioactivity removed during water sampling. R_{Total} was therefore equal to the total radioactivity present in the crab at the start of the washout period. As the cumulative radioactivity appearance in the water at every sampling time was measured, the radioactivity remaining in the crab at each (R_{Time}) could be back-calculated. R_{Time} data were natural-log transformed and regressed against time (on a linear scale) to yield the rate constant of diffusive water exchange (k, h^{-1}) as the slope of the line (Evans 1967) as follows:

$$k = \left(\ln R_{Time1} - \ln R_{Time2}\right)/\left(T_1 - T_2\right), \tag{11}$$

where R_{Time1} and R_{Time2} are total ^3H_2O radioactivity (in cpm) in the crab at times T_1 and T_2 (in h). In practice, regressions were performed over both the first 30 min and the first 90 min of washout (see "Results").

The exchangeable water pool (V_{H2O}—mL kg^{-1}) was calculated as:

$$V_{H2O} = R_{total}/\left(SA_{H2O} \times W\right), \tag{12}$$

where SA_{H2O} is the specific activity (cpm mL^{-1}) of the external water at the end of the ^3H_2O loading period and W is the crab weight in kg.

The unidirectional diffusive water flux rate (J_{H2O}, mL kg h^{-1}) was calculated from the k and V_{H2O} data:

$$J_{H2O} = -k \times V_{H2O}. \tag{13}$$

Statistical analysis

The tests of Shapiro–Wilks and Bartlett were performed to confirm data normality and homogeneity of variance, respectively. One-way analysis of variance, followed by Tukey's test, was used to determinate significant differences among treatments for all data ($p < 0.05$) using SigmaStat™ 3.5 (Systat Software Inc., San Jose, CA, USA). Paired Student's t tests (two-tailed) were used to evaluate differences between ΔH^+_m and Δlactate in the same crabs, and between simultaneous hemolymph and seawater ion concentrations for the same crabs at each salinity. SigmaPlot™ 11.0 (Systat Software Inc., San Jose, CA, USA) was used to graphically portray the data. All data are presented as means ± SEM (N).

Results

All crabs survived 7+ days across the range of salinities tested (10–50 ppt), though initial trials at higher (60 ppt) and lower salinities (5 ppt) resulted in mortalities (15–25%) during the acclimation period.

Experimental series 1: effects of acclimation to different salinities on metabolic, ionoregulatory, and acid–base parameters

Acclimation to different water salinities significantly changed the routine rates of oxygen uptake ($\dot{M}O_2$), ammonia excretion (Jamm), and urea-N excretion (Jurea-N), as well as calculated nitrogen quotient (NQ) (Fig. 1). Compared to the mean value in the control group at 32 ppt (989 µmol O_2 kg h^{-1}), $\dot{M}O_2$ was elevated by 62% at 10 ppt ($p < 0.05$). However, salinities varying from 20 to 50 ppt did not significantly affect $\dot{M}O_2$ (Fig. 1A). Jamm presented a threefold increase at 10 ppt ($p < 0.05$) when compared to the control (− 62 µmol N kg h^{-1}) (Fig. 1B). Similar to $\dot{M}O_2$, there were no differences ($p > 0.05$) in Jamm from 20 to 50 ppt (Fig. 1B). Jurea-N was − 4 µmol N kg h^{-1} under control conditions, amounting to only about 5% of the total N excretion ($\dot{M}_N$). Jurea-N presented a different response pattern than Jamm when salinity was above or below 32 ppt (Fig. 1C). At 40 and 50 ppt Jurea-N increased more than threefold ($p < 0.05$), respectively, when compared to the control group. The two- to threefold increases in Jurea-N at 20 ppt and 10 ppt were not statistically significant (Fig. 1C). The calculated nitrogen quotient (NQ = 0.06 under control conditions) presented the same pattern as Jamm, indicating a prominent 3.7-fold increase ($p < 0.05$) in the oxidation of nitrogen-containing fuels at 10 ppt, when compared the other salinities (Fig. 1D).

The mean control concentration of hemolymph total ammonia (T_{Amm} = 31.5 µmol L^{-1}) was not significantly altered by acclimation to higher or lower salinities (Fig. 2A). However, fractionation of T_{Amm} into its [NH_3] and [NH_4^+]

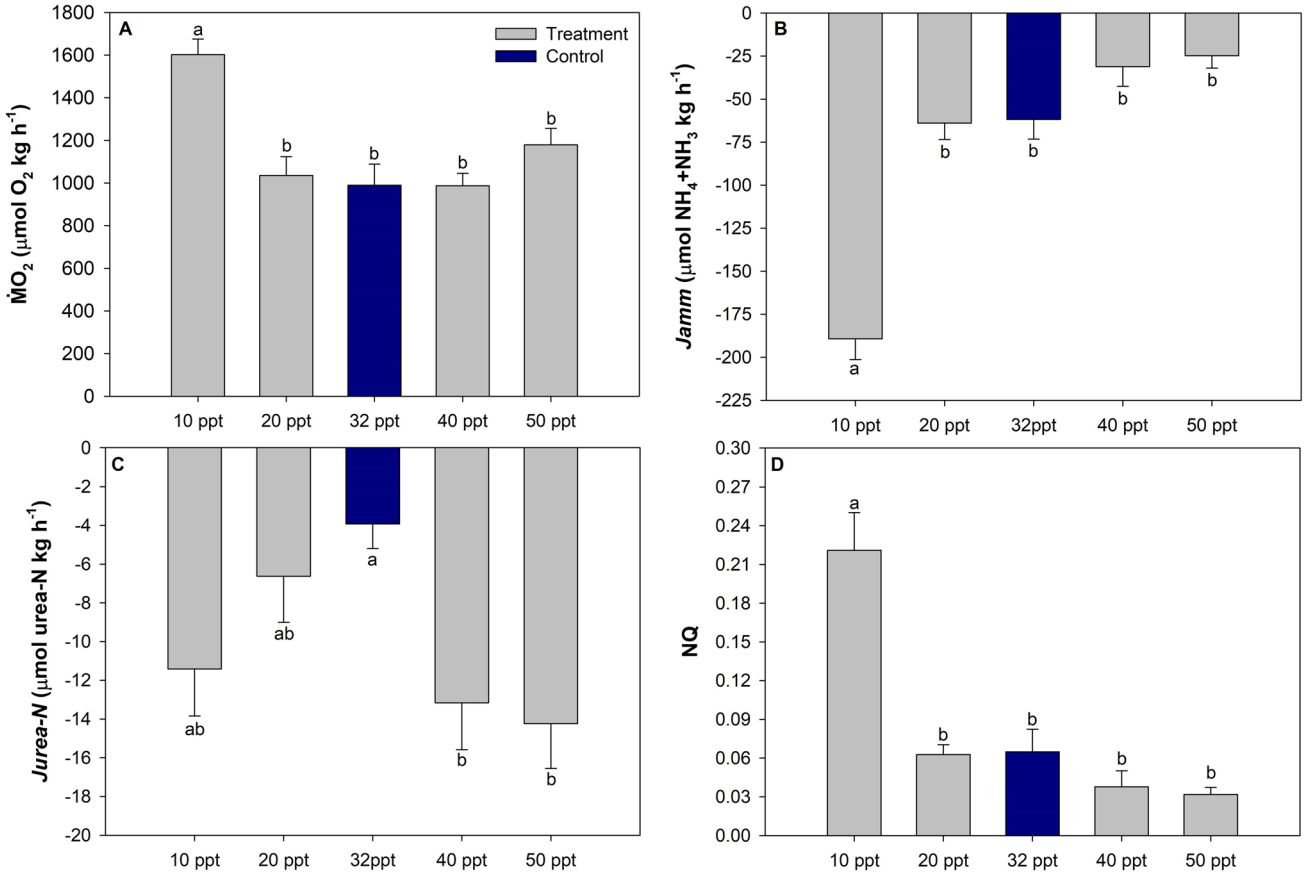

Fig. 1 Mean ± SEM ($N = 8$) values of **A** oxygen consumption rate ($\dot{M}O_2$—µmol O_2 kg^{-1} h^{-1}), **B** total ammonia flux rate (Jamm—µmol NH_4 + NH_3 kg^{-1} h^{-1}), **C** urea-N flux rate (Jurea-N—µmol urea-N kg^{-1} h^{-1}), and **D** calculated nitrogen quotient (NQ) of green crab (*Carcinus maenas*) acclimated to different water salinities [10, 20, 32 (control), 40 or 50 ppt] for 7 days. Letters indicate differences among treatments (one-way ANOVA, Tukey's test, $p < 0.05$)

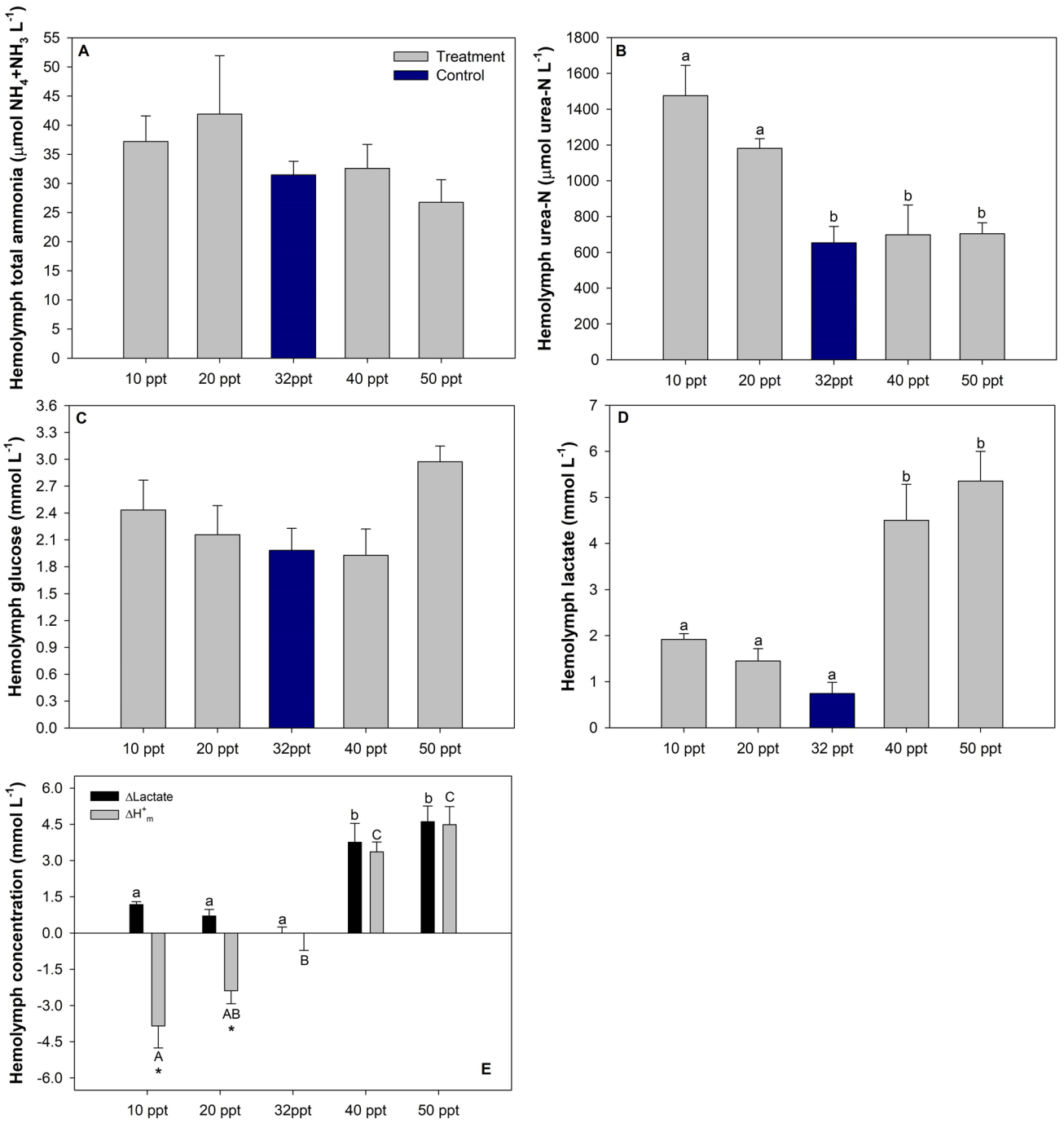

Fig. 2 Mean ± SEM ($N = 8$) values of **A** hemolymph total ammonia (T_{Amm}—μmol $NH_4^+ + NH_3$ L^{-1}), **B** urea-N (μmol urea-N L^{-1}), **C** glucose (mmol L^{-1}), **D** lactate (mmol L^{-1}), and **E** metabolic acid (positive) or metabolic base (negative) equivalents (ΔH_m^+) and Δlactate of green crab (*Carcinus maenas*) acclimated to different water salinities [10, 20, 32 (control), 40 or 50 ppt] for 7 days. Letters indicate differences among treatments (one-way ANOVA, Tukey's test, $p < 0.05$). When differences were not detected ($p > 0.05$), letters were omitted

components by Eqs. (5) and (6) and calculation of PNH_3 by Eq. (7) revealed a trend for increasing $[NH_3]$ and PNH_3 below 32 ppt, with constancy at higher salinities (Table 1). Hemolymph PNH_3 approximately doubled between 32 ppt (6.7 μTorr) and 10 ppt (14.4 μTorr), a significant increase. The $[NH_4^+]$ component was not significantly altered by salinity, remaining more than 98% of the total at all salinities.

The concentration of urea-N (654 μmol-N L^{-1}) in the control group (Fig. 2B) was about 20-fold higher than that

Table 1 Mean ± SEM ($N = 8$) value concentrations of NH_4^+ (μmol L^{-1}) and NH_3 (μmol L^{-1}), and the partial pressure of NH_3 (PNH_3 in μTorr) in the hemolymph of green crabs (*Carcinus maenas*) acclimated to different water salinities [10, 20, 32 (control), 40 or 50 ppt] for 7 days

Parameter	Water salinity				
	10 ppt	20 ppt	32 ppt	40 ppt	50 ppt
$[NH_4^+]$	36.63 ± 4.41	41.27 ± 9.91	31.09 ± 2.31	32.34 ± 4.07	26.5 ± 3.84
$[NH_3]$	0.79 ± 0.13^{A}	0.61 ± 0.13^{A}	0.37 ± 0.04^{AB}	0.25 ± 0.04^{B}	0.25 ± 0.03^{B}
PNH_3	14.41 ± 2.39^{A}	11.19 ± 2.37^{A}	6.73 ± 0.08^{AB}	4.56 ± 0.77^{B}	4.67 ± 0.66^{B}

Values for individual crabs were calculated from measurements of hemolymph total ammonia (T_{Amm}) concentrations (Fig. 2A) and pH (Fig. 3A) using Eqs. (5), (6), and (7). Letters indicate differences among treatments (one-way ANOVA, Tukey's test, $p < 0.05$). When differences were not detected ($p > 0.05$), letters were omitted

of total ammonia (T_{Amm}) in the hemolymph (Fig. 2A), despite the opposite disparity in their excretion rates (cf. Fig. 1B, C). Hemolymph urea-N levels increased 2.3- and 1.8-fold at 10 and 20 ppt ($p < 0.05$), respectively, when compared to the control. At 40 and 50 ppt, urea-N remained around control levels ($p > 0.05$) (Fig. 2B). At 32 ppt, the control glucose concentration in the hemolymph was 1.98 mmol L^{-1}; this did not change significantly with salinity, despite a 45% increase in the mean at 50 ppt (Fig. 2C). The mean value of hemolymph lactate at 32 ppt was 0.74 mmol L^{-1} (Fig. 2D). In contrast to the relative constancy in hemolymph glucose across salinities (Fig. 2C), lactate presented significant sixfold and sevenfold increases at 40 ppt and 50 ppt, respectively, but there were no significant differences across lower salinities (Fig. 2D). Salinity played an important role in the accumulation of metabolic (i.e., non-respiratory) acidic and basic equivalents in the hemolymph (Fig. 2E). At 10 ppt, the mean calculated ΔH^+_m was − 3.80 mmol L^{-1}, indicating an accumulation of metabolic base. As salinity increased, ΔH^+_m also increased, transitioning to positive values (metabolic acid accumulation) at salinities above 32 ppt, reaching 4.50 mmol L^{-1} at 50 ppt (Fig. 2E). Paired comparisons in individual crabs indicated significantly different (lower) values of ΔH_m^+ relative to Δlactate (elevation above mean control lactate concentration at 32 ppt) only at 10 and 20 ppt. Plasma total protein (mean control value at 32 ppt = 45.4 mg mL^{-1}) and amino acids concentrations (8.4 mmol L^{-1}) were not affected by salinity ($p > 0.05$) (Table 2).

Water pH was significantly lower at 10 and 20 ppt ($p < 0.05$) when compared to the mean control value (7.59) at 32 ppt, but there were no significant differences at 40 and 50 ppt ($p > 0.05$) (Table 2). Under control conditions, mean hemolymph pH was 7.85 and an increasing trend was observed at lower salinities, with significant differences at 10 ppt versus 32, 40 and 50 ppt (Fig. 3A). Hemolymph PCO_2, on the other hand, decreased at higher salinities. Under control conditions, mean PCO_2 was 2.94 Torr and this value dropped to 1.70 at 50 ppt ($p < 0.05$) (Fig. 3B). Differently from the patterns for pH and PCO_2 that tended to increase only at lower salinities (pH, Fig. 3A) or decrease at higher salinities (PCO_2, Fig. 3B), respectively, the $[HCO_3^-]$ concentrations in the hemolymph (Fig. 3C) presented a progressive decrease as salinity increased ($p < 0.05$). Compared to the mean value in the control group (9.85 mmol L^{-1}), the hemolymph $[HCO_3^-]$ increased by 27% and 23% at 10 and 20 ppt, and decreased by 31% and 43% at 40 and 50 ppt, respectively (Fig. 3C). A Davenport (1974) diagram relating pH, $[HCO_3^-]$, and PCO_2 is shown in Fig. 3D, based on constants reported for *C. maenas* by Truchot (1976a) with the non-bicarbonate buffer line (NBB) calculated from the β versus hemolymph protein regression of Truchot (1976b) plotted through the control data at 32 ppt. Compared to the control, the exposure to 10 and 20 ppt resulted in titration of hemolymph in an alkalotic direction roughly along the

Table 2 Mean ± SEM ($N = 8$) values of water pH, hemolymph concentrations of amino acids (mmol L^{-1}), and total protein (mg mL^{-1}) of green crab (*Carcinus maenas*) acclimated to different water salinities [10, 20, 32 (control), 40 or 50 ppt] for 7 days

Parameter	Matrix	Water salinity				
		10 ppt	20 ppt	32 ppt	40 ppt	50 ppt
pH	Water	7.19 ± 0.05^{A}	7.39 ± 0.06^{B}	7.59 ± 0.04^{C}	7.70 ± 0.03^{C}	7.67 ± 0.04^{C}
Total protein	Hemolymph	52.87 ± 1.79	43.29 ± 4.12	45.43 ± 2.98	44.92 ± 3.55	44.02 ± 3.79
Amino acids		8.10 ± 0.57	8.80 ± 0.97	8.38 ± 0.44	8.41 ± 0.44	8.22 ± 0.50

Letters indicate differences among treatments (one-way ANOVA, Tukey's test, $p < 0.05$). When differences were not detected ($p > 0.05$) letters were omitted

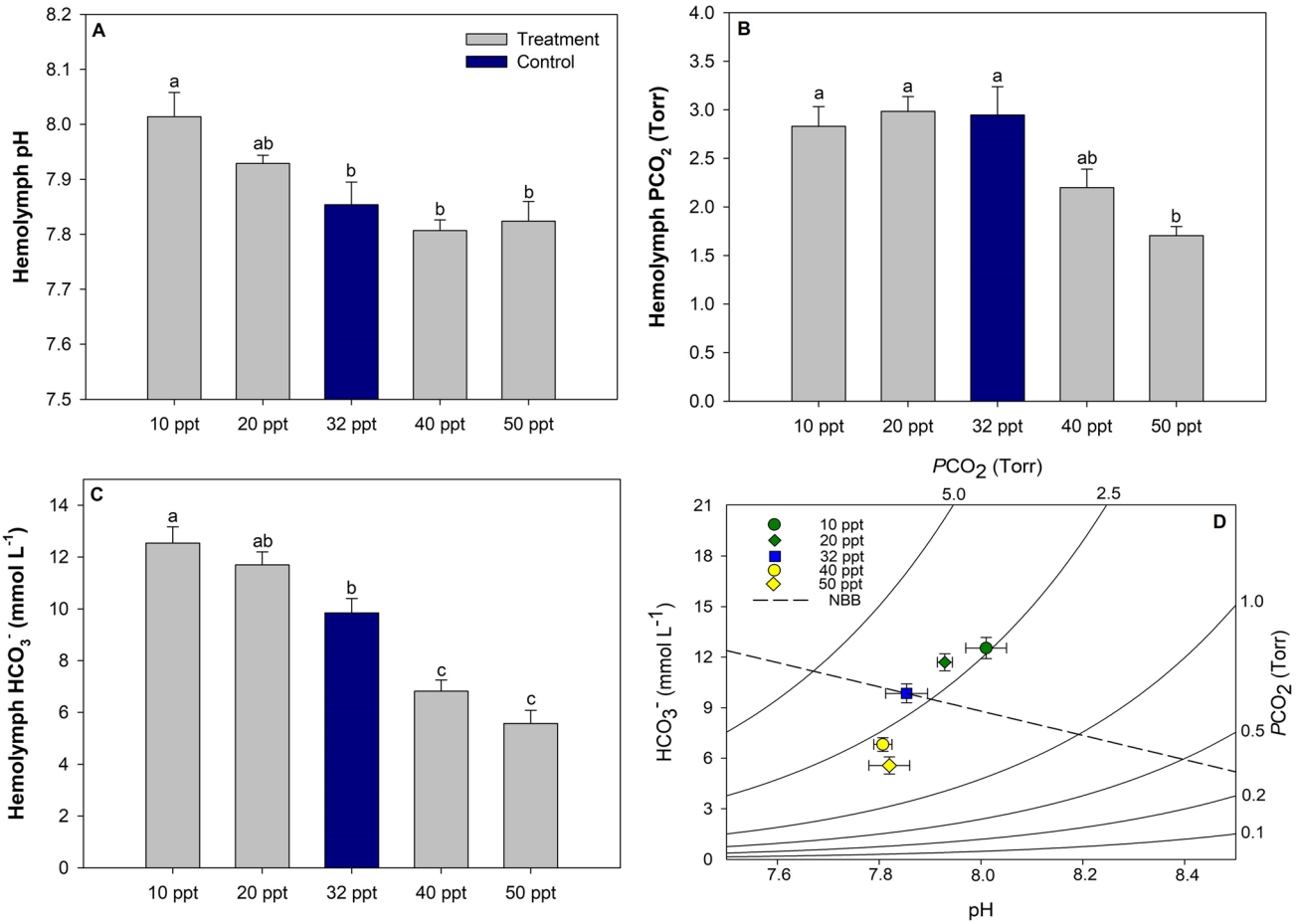

Fig. 3 Mean ± SEM ($N = 8$) values of **A** hemolymph pH, **B** CO_2 partial pressure (PCO_2—Torr), **C** bicarbonate (HCO_3^-—mmol L^{-1}), and **D** pH/HCO_3^- diagram, or Davenport diagram (Davenport 1974) of green crab (*Carcinus maenas*) acclimated to different water salinities [10, 20, 32 (control), 40 or 50 ppt] for 7 days. Letters indicate differences among treatments (one-way ANOVA, Tukey's test, $p < 0.05$). The dashed straight line in (**D**) is the non-bicarbonate buffer line (NBB) calculated according to Truchot (1976b). pK and αCO2 for *Carcinus maenas* were obtained from Truchot (1976a)

2.5 Torr PCO_2 isopleth. At this scenario, both treatments were above the NBB line, which is consistent with gains in hemolymph base (as [HCO_3^-]), as calculated in Fig. 2E—i.e., simple metabolic alkalosis. When salinity increased above the 32 ppt control level, an activation of anaerobic metabolism and a state of metabolic acidosis (decreased [HCO_3^-], consistent with Fig. 2E) and increased [lactate] (Fig. 2D), in combination with respiratory compensation (decreased PCO_2), were detected (Fig. 3D).

Figure 4 presents the paired individual values of water and hemolymph [ions] and osmolality; significant differences between the hemolymph and the environment are marked with asterisks. The mean [Cl^-] in the hemolymph (491 mmol L^{-1}) was maintained around seawater levels (505 mmol L^{-1}) when crabs were kept at 32 ppt ($p > 0.05$). At lower and higher salinities, we detected effective up- and down-regulation so as to keep hemolymph [Cl^-] closer to control conditions than in the external seawater (Fig. 4A). These differences were significant at 10 and 20 ppt (hemolymph [Cl^-] > seawater [Cl^-] by 130–102 mmol L^{-1}) and at 40 and 50 ppt (hemolymph [Cl^-] < seawater [Cl^-] by 105–122 mmol L^{-1}). The pattern was somewhat different for [Na^+] (Fig. 4B). At 32 ppt, mean [Na^+] in the hemolymph (364 mmol L^{-1}) was maintained near seawater values (345 mmol L^{-1}). As for [Cl^-], when salinity was decreased to 10 and 20 ppt, the crabs exhibited hyper-regulation of hemolymph [Na^+], keeping it significantly above environmental levels by 151–110 mmol L^{-1}). However, in contrast to [Cl^-], hyper-regulation of hemolymph [Na^+] also occurred at higher salinities, and was significant at 50 ppt by 161 mmol L^{-1}) (Fig. 4B). Hemolymph [K^+] (mean = 12.7 mmol L^{-1}at 32 ppt) exhibited yet another pattern, being hyper-regulated significantly above environmental concentrations at all salinities except 50 ppt, with the greatest differences (up to 3.9 mmol L^{-1}) at the lowest salinities (Fig. 4C). The pattern for hemolymph [Ca^{2+}]

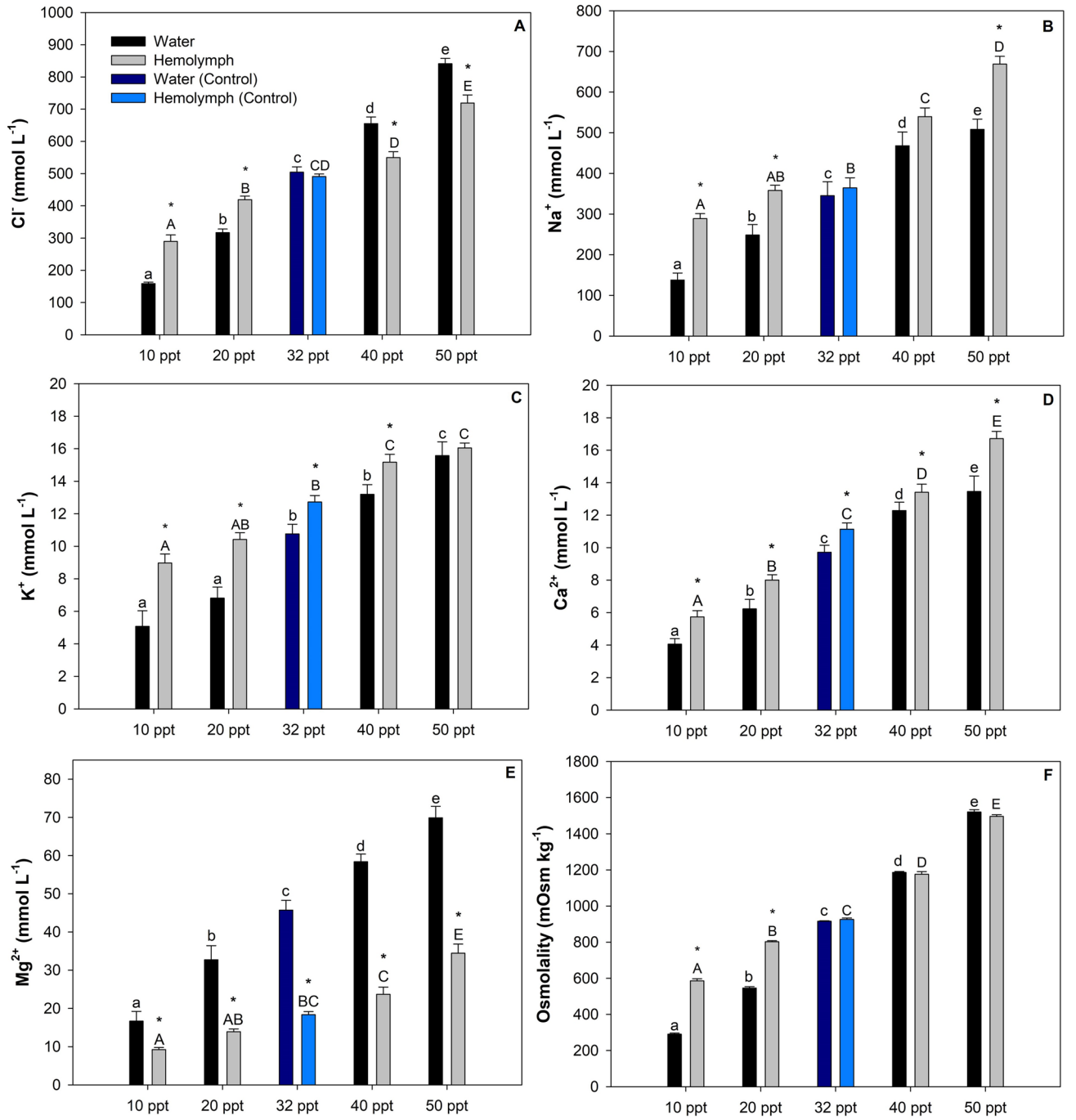

Fig. 4 Mean ± SEM ($N = 8$) concentrations of water and hemolymph **A** chloride (Cl^-—mmol L^{-1}), **B** sodium (Na^+—mmol L^{-1}), **C** potassium (K^+—mmol L^{-1}), **D** calcium (Ca^{2+}—mmol L^{-1}), **E** magnesium (Mg^{2+}—mmol L^{-1}) and **F** values of osmolality (mOsm—kg^{-1}) for the green crab (*Carcinus maenas*) acclimated to different water salinities [10, 20, 32 (control), 40 or 50 ppt] for 7 days. Lowercase letters indicate differences in water among treatments and capitalized letters indicate differences in hemolymph among treatments (one-way ANOVA, Tukey's test, $p < 0.05$). Asterisks indicates differences between water and hemolymph within the same treatment/salinity (paired t test, $p < 0.05$). When significant differences were not detected ($p > 0.05$), letters/symbols were omitted

(mean = 11.1 mmol L^{-1}at 32 ppt) was similar to that for [K^+], with significant hyper-regulation at all salinities, even at 50 ppt (Fig. 4D). These differences ranged from 1.7 to 3.3 mmol L^{-1}. The most impressive regulation of all was that for hemolymph [Mg^{2+}] (mean = 18.4 mmol L^{-1}at 32 ppt), which was significantly hypo-regulated by about 35–50% at all salinities, with the greatest absolute difference (35.5 mmol L^{-1}) at 50 ppt (Fig. 4E). With respect to

osmolality, at 32, 40 and 50 ppt crabs displayed an efficient osmoconforming strategy, with similar values for plasma and seawater (Fig. 4F). For example, mean control hemolymph osmolality was 926 mOsm kg^{-1} whereas that for 32 ppt seawater was 916 mOsm kg^{-1}. At 10 and 20 ppt, on the other hand, significant hyper-regulation occurred; the crabs kept hemolymph osmolality higher than seawater values by 102% and 47%, differences amounting to 296 and 256 mOsm kg^{-1} respectively.

Experimental series 2: transepithelial potential (TEP)

At 32 ppt, the mean control TEP was − 1.12 mV relative to the external seawater. Crabs exhibited a progressively upward trend to less negative TEP values along with the increase of salinity (Fig. 5). Compared to the control, absolute TEP decreased by 28% and 58% in crabs at 40 and 50 ppt, whereas at 10 and 20 ppt, absolute TEP increased by 50% and 64% compared to the control group. As a result, animals acclimated to the lower range of salinities (10 and 20 ppt) presented significantly more negative TEP values ($p < 0.05$) when compared to those at higher salinity (40 and 50 ppt) (Fig. 5).

Experimental series 3: diffusive water fluxes

At 32 ppt, the mean diffusive water exchange rate constant (k, h^{-1}) calculated over 30 min of washout was 0.71 h^{-1} (i.e., 71% of the exchangeable body water pool per hour) and significantly increased to 1.04 h^{-1} in crabs acclimated to 50 ppt ($p < 0.05$) (Fig. 6A). Values calculated over 90 min of washout tended to be slightly lower by a few %, but

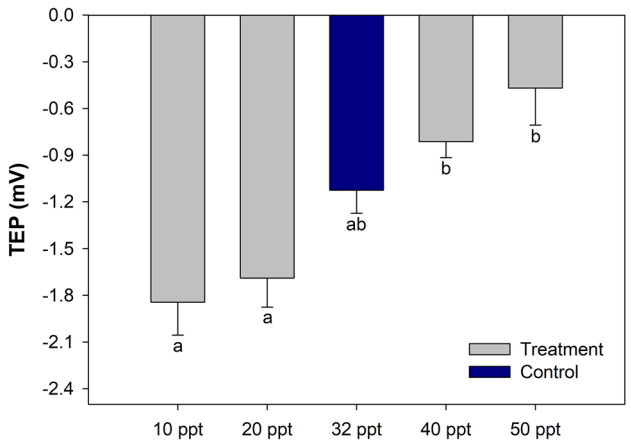

Fig. 5 Mean ± SEM ($N = 8$) values of the trans-epithelial potential (TEP—mV) of green crab (*Carcinus maenas*) acclimated to different water salinities [10, 20, 32 (control), 40 or 50 ppt] for 7 days. Letters indicate differences among treatments (one-way ANOVA, Tukey's test, $p < 0.05$)

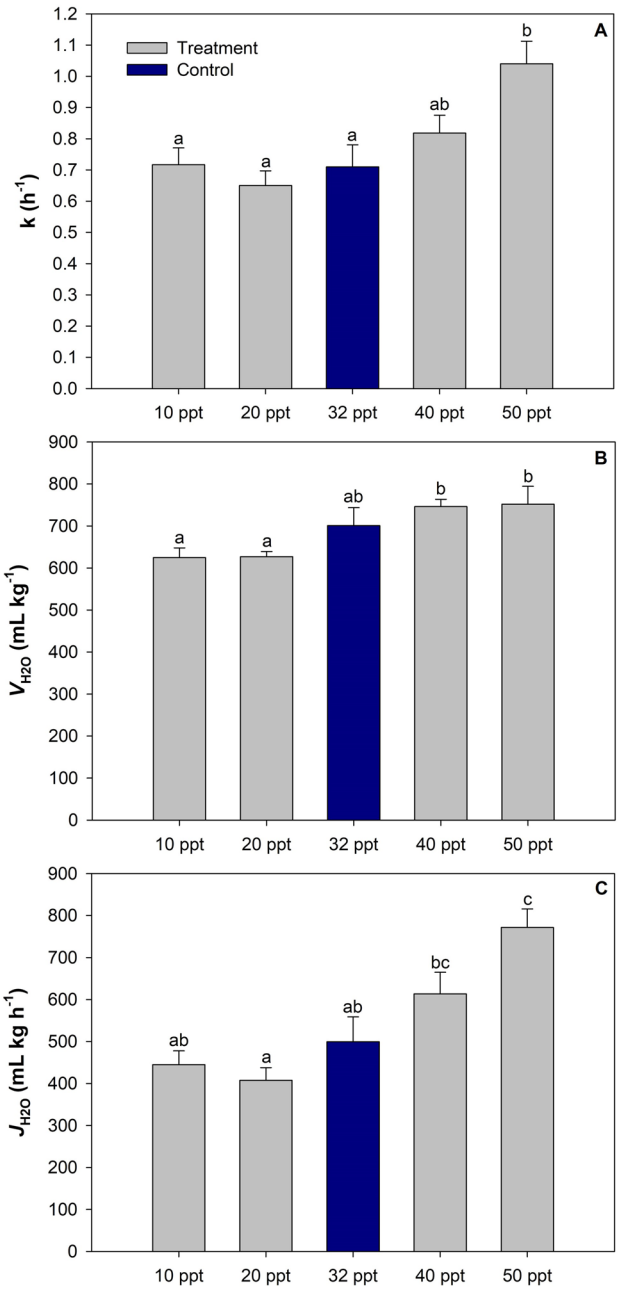

Fig. 6 Mean ± SEM ($N = 8$–14) values of **A** the rate constant of diffusive water exchange (k—h^{-1}), **B** the exchangeable water pool (V_{H2O}—mL kg^{-1}), and **C** the unidirectional diffusive water flux rate (J_{H2O}—mL kg^{-1} h^{-1}) of green crab (*Carcinus maenas*) acclimated to different water salinities [10, 20, 32 (control), 40 or 50 ppt] for 7 days. Letters indicate differences among treatments (One-way ANOVA, Tukey's test, $p < 0.05$)

not significantly different from those calculated over 30 min at any salinity. In the control group at 32 ppt, the mean exchangeable body water pool (V_{H2O}) was 701 mL kg^{-1}. Crabs in the 10 and 20 ppt treatments presented V_{H2O} values about 12% lower when compared the animals acclimated at 32 ppt, whereas V_{H2O} values at 40 and 50 ppt were about

7% higher; the values at the two lower salinities were significantly different ($p < 0.05$) from those at the two higher salinities (Fig. 6B). These k and V_{H2O} values resulted in a mean unidirectional diffusive water flux rate (J_{H2O}) of 499 mL kg h^{-1} at 32 ppt. When compared to the control group, J_{H2O} exhibited an increasing trend at higher salinities that became significant at 50 ppt ($p < 0.001$) where the mean rate reached 771 mL kg h^{-1} (Fig. 6C). Acclimation to lower salinities did not affect J_{H2O} ($p > 0.05$).

Discussion

While the green crab tolerated a salinity range of 10–50 ppt without mortality, it exhibited a host of internal physiological disturbances in virtually all of the measured parameters, many of which were interrelated. The most extreme of these occurred at the lower and upper ends of the range. Three in particular may be limiting: a severe disturbance in N metabolism and fuel usage at low salinity, the appearance of lactacidosis at high salinity, as well as elevated hemolymph [Mg^{2+}] at high salinity.

O_2 consumption and nitrogen metabolism

Control $\dot{M}O_2$ at 32 ppt (989 µmol kg^{-1} h^{-1}; Fig. 1A) was typical of many previous measurements on resting green crabs under similar conditions (Taylor et al. 1977; Johnson and Uglow 1985; Wilson et al. 2021). Control Jamm values (− 62 µmol N kg h^{-1}; Fig. 1B) were comparable to those recently reported by Quijada-Rodriguez et al. (2022) for similarly fasted animals, but somewhat lower than most other previous reports (Spaargaren 1982; Simonik and Henry 2014; Weihrauch et al. 1999; Durand and Regnault 1998); this difference may relate to feeding history. The control Jurea-N values (− 4 µmol N kg h^{-1}; Fig. 1C) also agreed with very low rates reported by Quijada-Rodriguez et al. (2022) for fasted crabs under similar conditions. There are only a few other previous measurements of Jurea-N in *C. maenas* (Durand and Regnault 1998; Weihrauch et al. 1999) and these agree that it is low relative to Jamm.

The marked increases in both $\dot{M}O_2$ (Fig. 1A) and Jamm (Fig. 1B) observed at low salinity agree with previous reports on *C. maenas* for $\dot{M}O_2$ (Siebers et al. 1972; Taylor 1977) and Jamm (Spaargaren 1982) and show that the threshold for both responses is below 20 ppt. Jurea-N also tended to increase at low salinity (Fig. 1C). Clearly, metabolic costs were elevated at 10 ppt, and part of these may be the cost of hyperosmotic regulation, as discussed subsequently, though a general stress response may also be involved. Another possible explanation is the behavioral increase of locomotor activity of *C. maenas* in low salinity which occurs in the short term—also known as halokinesis (McGaw et al 1999). However, during our measurements on 7-day exposed crabs, we did not detect halokinetic behavior. We are aware of no previous measurements of these parameters under hypersaline conditions in green crabs; the present data indicate that both $\dot{M}O_2$ and Jamm remain unchanged at 40 and 50 ppt (Fig. 1A, B). This is surprising, inasmuch as there was evidence for greater reliance on anaerobic metabolism, with increased hemolymph concentrations of both lactate (Fig. 2D) and ΔH_m^+ (Fig. 2E) at these high salinities. The concentration of hemolymph glucose, on the other hand, presented no significant alteration through all tested salinities (Fig. 2C). In experimental anoxic conditions, a marked elevation of hemolymph lactate of *C. maenas* was reported by Hill et al. (1991). In the same paper, a reduction in the whole-body glycogen concentration followed by an increase of glucose oligosaccharides in the muscle, but no alteration on the hemolymph free glucose was observed. The authors suggested that anaerobic glycolysis could be an important source of lactate as a metabolic substrate and that free glucose would either play an unimportant role in the anaerobic metabolism or that *C. maenas* precisely controls its concentration. Interestingly, Jurea-N increased markedly at 40 and 50 ppt (Fig. 1C). This could reflect degradation of ATP stores, with the purine ring component of the adenylate being metabolized to urea-N. Perhaps, other factors constrain the ability to elevate $\dot{M}O_2$ under these circumstances, so that the crab turns to anaerobic metabolism to satisfy increased costs.

The NQ under control conditions (0.06; Fig. 1D) was similar to the value (0.04) that can be calculated from the data of Simonik and Henry (2014) for green crabs in similar circumstances, though these authors reported much higher absolute values for both $\dot{M}O_2$ and Jamm, and did not measure Jurea-N. By metabolic theory, the AQ would be 0.27 if all aerobic metabolism were fueled by the oxidation of N-containing substrates such as amino acids and purines (Lauff and Wood 1996; Wang et al. 2021), so a control AQ of 0.06 would indicate that only 22% of resting metabolism was based on such fuels. However, at 10 ppt, the AQ was elevated markedly to 0.22 (Fig. 1D), indicating that this contribution increased to 81%. Such a high reliance on endogenous N-substrates would likely cause protein depletion and prevent growth at 10 ppt unless an abundant food supply were available, raising questions about the long-term survival of *C. maenas* at 10 ppt.

The present hemolymph T_{Amm} value under control conditions (31.5 µmol L^{-1}; Fig. 2A) appears to be lowest ever recorded for *C. maenas*, with other reports ranging from 81 to 940 µmol L^{-1}, whereas control hemolymph urea-N concentration (654 µmol-N L^{-1}; Fig. 1B) was in the mid-range (48–1760 µmol-N L^{-1}) of previous measurements (Binns 1969; Spaargaren 1982; Durand and Regnault 1998; Weihrauch et al. 1999, 2017; Simonik and Henry 2014;

Quijada-Rodriguez et al. 2022). Again, these wide variations among studies may relate to different feeding histories (Weihrauch et al. 2017), molt status, age, size, and sex (McGaw et al. 1992). While there was no significant variation in hemolymph T_{Amm} across acclimation salinities (Fig. 2A), the fractionation calculations revealed that the $[NH_3]$ component, and therefore also PNH_3, increased as salinity decreased (Table 2). In large part, this was due to the rise in hemolymph pH in crabs acclimated to 10 and 20 ppt (Fig. 3A, D), but the decrease in pK associated with the lower ionic strength of the hemolymph (see Eq. 5) also made a contribution (Cameron and Heisler 1983). As internal PNH_3 provides the driving force for the diffusive excretion of NH_3 across the gills, the approximate doubling of PNH_3 between 32 and 10 ppt (Table 1) probably made an important contribution to the tripling of Jamm at 10 ppt (Fig. 1B). However, one or more active transport processes for ammonia, powered by Na^+, K^+ ATPase and linked in some way to the active Na^+ uptake, needed for hyper-osmoregulation at low salinity may also have contributed to the greatly elevated Jamm at 10 ppt (Weihrauch et al. 1999, 2017).

Acid–base balance

The pattern of metabolic alkalosis (elevated pH and $[HCO_3^-]$) with unchanged PCO_2 (Fig. 3) in green crabs acclimated to 10 and 20 ppt is in accord with previous reports on the same species (Zanders 1980; Truchot 1973, 1981). In the present study, increased pH and $[HCO_3^-]$ occurred despite a decrease in water pH at low salinity (Table 2), and while water $[HCO_3^-]$ was not measured, it undoubtedly fell as well, because salinities of 10 and 20 ppt were obtained by diluting BMSC seawater ($[HCO_3^-]$ = approximately 2 mmol L^{-1}) with BMSC freshwater ($[HCO_3^-]$ = approximately 0.04 mmol L^{-1}). As discussed extensively by Truchot (1987), metabolic alkalosis is an almost universal pattern for euryhaline invertebrates (and some vertebrates) when exposed to dilute salinity, but the explanation is not clear. Most likely, it is a secondary consequence of changes in the strong ion difference (SID) (Stewart 1978) in the hemolymph, linked to differential changes in the concentrations of strong cations versus strong anions. Given the high ion concentrations in crab hemolymph and limitations of analytical precision, this SID change of a few mmol L^{-1} would be very difficult to measure directly, but was reflected in the negative ΔH_m^+ values at 10 and 20 ppt (Fig. 2E). The response has clear adaptive significance, because the higher pH will counter the unfavorable effect of dilute ionic strength on the oxygen affinity of hemocyanin (Truchot 1973), thereby protecting blood O_2 transport, at a time when the metabolic rate is increased (Fig. 1A).

There appear to be no previous reports of the acid–base response to hypersaline exposure in *C. maenas*. In the present study, while hemolymph pH did not change, the trend for a negative relationship between hemolymph $[HCO_3^-]$ and salinity continued above 32 ppt (Fig. 3C). However, the mechanism appeared to be different, reflecting the activation of anaerobic metabolism with equimolar increases in ΔH^+_m and Δlactate concentrations (Fig. 2D, E)—classic metabolic acidosis with some respiratory compensation (decreased hemolymph PCO_2, Fig. 3B, D). Ongoing anaerobic metabolism and associated lactacidosis would cause wastage of metabolic fuels, and would be problematical for long-term health of the green crab at high salinity. In air breathers, the respiratory compensation which stabilizes pH in the face of metabolic acidosis would be attributed to hyperventilation. However, the ability of water breathers to change internal PCO_2 levels by ventilation is generally considered to be rather limited (Dejours 1981; Henry et al. 2012), though lower PCO_2 associated with hyperventilation has been observed in the green crabs exposed to chronic hypoxia (Taylor 1982; Truchot 1987). $\dot{M}O_2$ did not increase at 40 and 50 ppt (Fig. 1A), which argues against hyperventilation. As discussed below, the narcotic effect associated with the elevated hemolymph $[Mg^{2+}]$ (Fig. 4E) may have played a role here. An alternate explanation could be the greater alkalinity and buffer capacity of seawater at higher salinity, Seawater $[HCO_3^-]$ would increase from 2.0 mmol L^{-1} at 32 ppt to about 2.6 and 3.1 mmol L^{-1} at 40 and 50 ppt respectively. This would effectively increase its CO_2 capacitance coefficient, making it a stronger "sink" for CO_2, thereby lowering hemolymph PCO_2 (Truchot 1981, 1987; Truchot and Forgue 1998). In future, direct measurements of ventilation at high salinity would be helpful in clarifying the situation.

Ionoregulation and osmoregulation

Our data on the regulation of hemolymph ions and osmolality at 10, 20, and 32 ppt (Fig. 4) were consistent, both quantitatively and qualitatively, with many previous reports on *C. maenas* (Bateman 1933; Webb 1940; Zanders 1980; Siebers et al. 1982). The principal feature was progressive hyper-regulation of hemolymph osmolality, $[Na^+]$, and $[Cl^-]$ at salinities below 32 ppt; Henry et al. (2012) identified the threshold for the start of hyper-regulation at about 26 ppt. In addition, the hyper-regulation of $[K^+]$ and $[Ca^{2+}]$ that was already present at 32 ppt continued at lower salinities, as did the hypo-regulation of $[Mg^{2+}]$ that was also already present in crabs acclimated to 32 ppt. There is an extensive literature on the mechanisms of $[Na^+]$, $[K^+]$, $[Ca^{2+}]$ and $[Cl^-]$ hyper-regulation at low salinity in the green crab and other decapods (Freire et al. 2008; Henry et al. 2012; McNamara and Faria 2012). Active uptake from the water by the posterior gills appears to be the primary mechanism of regulation of these ions, though some reabsorption of Na^+,

K^+, and Cl^- from the urine also occurs. On the other hand, [Mg^{2+}] hypo-regulation appears to be mainly a function of excretion via the antennal gland involving active secretion into the urine (Morritt and Spicer 1993; Freire et al. 2008).

There is little prior information on the ionoregulatory responses of *C. maenas* to higher salinities. Our data concur with Siebers et al. (1982) and Zatta (1987) that osmoconformation occurs in green crabs at 40 and 50 ppt (Fig. 4F), but by carefully comparing simultaneous hemolymph and seawater samples, we found that [Na^+] was actually hyper-regulated (Fig. 4B) while [Cl^-] was hypo-regulated (Fig. 4A), an observation that requires future mechanistic investigation. Furthermore, the hyper-regulation of hemolymph [K^+] (Fig. 4C) and [Ca^{2+}] (Fig. 4D) and hypo-regulation of [Mg^{2+}] (Fig. 4E) continued at these higher salinities. Presumably, some or all of the same mechanisms identified at lower salinities were responsible, but again this requires future investigation. The hypo-regulation of [Mg^{2+}] was the most pronounced trend at high salinity (Fig. 4E), suggesting that this is critically important. Modest elevations of hemolymph [Mg^{2+}] in *C. maenas* have beneficial effects such as improving the O_2 affinity of hemocyanin and its ability to deliver O_2 to the tissues, the latter by enhancing the Bohr factor (Truchot 1975). However, large elevations of hemolymph [Mg^{2+}] are dangerous because they depress heart rate and have a general anesthetic effect on crabs (Frederich et al. 2000). At 50 ppt, hemolymph [Mg^{2+}] was almost twofold higher than at 32 ppt, and fourfold higher than at 10 ppt (Fig. 4E). Potentially, this may be a factor that limits the upper salinity tolerance of the green crab, as elevated hemolymph [Mg^{2+}] could depress the central nervous system, reducing ventilation and the delivery of O_2 to the tissues and thereby leading to anaerobiotic metabolism.

Transepithelial potential (TEP)

We detected a clear trend for TEP to become more negative as acclimation salinity was lowered and less negative as acclimation salinity was raised (Fig. 5). However, relative to the control value at 32 ppt (− 1.1 mV), none of the TEP differences were significant, though the values at 10 and 20 ppt were significantly different from those at 40 and 50 ppt. Three previous studies on *C. maenas* reported similar control values (− 0.5 to − 2.5 mV), but detected no change in TEP at reduced salinity (Greenaway 1976; Zanders 1980; Winkler 1986). All these results are very different from studies on perfused gills, where values became much more negative at reduced salinity, especially in the Na^+, K^+ ATPase-rich posterior gills (Siebers et al. 1986; Winkler 1986; Lucu and Siebers 1986). This reflects a negative electrogenic potential important in driving Na^+ uptake that is superimposed upon a diffusion potential that is also negative, due to a greater permeability of the gills to cations than anions (Siebers et al. 1985, 1989). These gill-specific TEPs may be somewhat dissipated when measured in the whole animal; nevertheless, the clear salinity-dependent trend observed (Fig. 5) likely reflected the combined responses of electrogenic and diffusion potentials. Future studies involving manipulations of individual ions will be instructive.

Water regulation

At the control salinity (32 ppt), the rate constant for diffusive water exchange (0.71 h^{-1}; Fig. 6A) was very similar to that reported in several other studies on *C. maenas* using comparable methods, temperatures, and salinity (Rudy 1967; Rasmussen and Bjerregaard 1995; Rasmussen and Andersen 1996). Our findings agree with Rudy (1967) in showing no detectable decrease in water permeability as acclimation salinity was reduced from 32 to 20 or 10 ppt, whereas Rasmussen and Bjerregaard (1995), Rasmussen and Andersen (1996), and several other studies using different methods (Smith 1970; Berlind and Kamemoto 1977; Rainbow and Black 2001) reported small, but significant decrements over this same range. No other studies on *C. maenas* have looked at the effects of acclimation to hypersaline conditions, where we found an increasing trend which became significant at 50 ppt (1.04 h^{-1}; Fig. 6A). It is notable that water permeability started to rise above 32 ppt, the same region where the crab becomes an osmoconformer, and that the region of plateau [present study and Rudy (1967)] or slight decrease (other studies) occurred in the lower salinity range (Fig. 6A) where the crab osmoregulates (Fig. 4F). Lowering diffusive water permeability may be beneficial in reducing the cost of osmoregulation at lower salinities, yet in itself, this may have negative effects on other processes. Therefore, relaxing this water permeability reduction may be beneficial at higher salinities when there is no longer a need to osmoregulate.

Our refinement of the diffusive water flux method allowed us to also measure the volume of the exchangeable water pool (V_{H2O}; Eq. 12). At 32 ppt, this value (701 mL kg^{-1}) was identical to the total body water content reported by Zatta (1987) in the same species at the same salinity, suggesting that all of the water in the body is exchangeable. From the product of V_{H2O} times k, the absolute unidirectional diffusive water flux rates were calculated (J_{H2O}; Eq. 13). These analyses revealed that V_{H2O} (Fig. 6B) followed the same general trend as the rate constant k (Fig. 6A), and therefore the increases in J_{H2O} at 40 and 50 ppt (Fig. 6C) were more marked than in either k or V_{H2O} alone. We are aware of no previous measurements of V_{H2O} as function of salinity in *C. maenas*, but Schwabe (1933) reported negligible changes in body weight when green crabs were transferred to lower salinities. There are also reports that that extracellular fluid volume (ECFV), which is normally about 320 mL kg^{-1} in 100% seawater (i.e., 46% of V_{H2O}), is stable over the lower

salinity range used in the present study, but increases in crabs acclimated to hypersaline conditions (52 ppt) (Zanders 1980; Harris and Andrews 1982). Overall, these data are in accord with the present trends in V_{H2O}. Harris and Andrews (1982) speculated that the increase in ECFV at high salinity was due to a redistribution of water between intracellular and extracellular compartments, while the present data suggest that there is an increase in the total body water content, though this remains to be proven.

Perspectives

The ability of *C. maenas* to tolerate a wide range of salinities is clearly an important contributor to its success as an invasive species (Behrens-Yamada 2001; Klassen and Locke 2007; Leignel et al. 2014). Most studies have highlighted its ability to give up the osmoconformation seen at high salinities, and to hyper-regulate most ions and osmolality when challenged with lower salinities. However, hidden inside this pattern there are many disturbances in a variety of physiological parameters, not only under hypo-saline exposure, but also under hyper-saline exposure. It is the ability of the species to tolerate such large perturbations of internal homeostasis that is remarkable.

Acknowledgements The authors thank the BMSC staff, especially research co-ordinators Eric Clelland and Tao Eastham, for their support, and we appreciate the constructive reviewer comments.

Authors' contribution The study was designed by all authors, and the experiments and measurements were performed by all authors. GDP and CMW wrote the first draft of the manuscript, JW and BP edited it, and all authors approved the final version.

Funding The study was funded by an NSERC (Canada) Discovery Grant (RGPIN-2017-03843) to CMW.

Declarations

Conflict of interest All authors declare that they have no conflict of interest.

Ethics approval Approval was obtained from Bamfield Marine Sciences Centre Invertebrate AUP RS-18-19; Fisheries and Oceans Canada Collection Permit XR 212 2019.

References

Bateman JB (1933) Osmotic and ionic regulation in the Shore Crab, *Carcinus maenas*, with notes on the blood concentrations of *Gammarus locusta* and *Ligia oceanica*. J Exp Biol 10(4):355–371

Behrens-Yamada S (2001) Global invader: the European green crab. Oregon State University, Corvallis

Berlind A, Kamemoto FI (1977) Rapid water permeability changes in eyestalkless euryhaline crabs and in isolated, perfused gills. Comp Biochem Physiol A Mol Integr Physiol 58(4):383–385

Binns R (1969) The physiology of the antennal gland of Carcinus maenas (L.) V. Some nitrogenous constituents in the blood and urine. J Exp Biol 51(1):41–45

Boutilier RG, Heming TA, Iwama GK (1984) Appendix: Physicochemical parameters for use in fish respiratory physiology. In: Hoar WS, Randall DJ (eds) Fish physiology, vol 10. Academic Press, pp 403–430

Bradford MM (1976) A rapid and sensitive method for the quantitation of microgram quantities of protein utilizing the principle of protein-dye binding. Anal Biochem 72(1):248–254

Cameron JN, Heisler N (1983) Studies of ammonia in the rainbow trout: physico-chemical parameters, acid–base behaviour and respiratory clearance. J Exp Biol 105(1):107–125

Dal Pont G, Souza-Bastos LR, Giacomin M, Dolatto RG, Baika LM, Grassi MT, Ostrensky A, Wood CM (2019) Acute exposure to the water-soluble fraction of gasoline (WSFG) affects oxygen consumption, nitrogenous-waste and Mg excretion, and activates anaerobic metabolism in the goldfish *Carassius auratus*. Comp Biochem Physiol C Toxicol Pharmacol 226:108590

Davenport HW (1974) The ABC of acid–base chemistry: the elements of physiological blood-gas chemistry for medical students and physicians. University of Chicago Press, Chicago

Dejours P (1981) Principles of comparative respiratory physiology, 2nd edn. Elsevier North-Holland, Amsterdam

Durand F, Regnault M (1998) Nitrogen metabolism of two portunid crabs, *Carcinus maenas* and *Necora puber*, during prolonged air exposure and subsequent recovery: a comparative study. J Exp Biol 201(17):2515–2528

Evans DH (1967) Sodium, chloride and water balance of the intertidal teleost, Xiphister Atropurpureus: III. The roles of simple diffusion, exchange diffusion, osmosis and active transport. J Exp Biol 47(3):525–534

Frederich M, Sartoris FJ, Arntz WE, Portner H (2000) Haemolymph Mg^{2+}regulation in decapod crustaceans: physiological correlates and ecological consequences in polar areas. J Exp Biol 203(8):1383–1393

Freire CA, Onken H, McNamara JC (2008) A structure–function analysis of ion transport in crustacean gills and excretory organs. Comp Biochem Physiol A Mol Integr Physiol 151(3):272–304

Giacomin M, Dal Pont G, Eom J, Schulte PM, Wood CM (2019a) The effects of salinity and hypoxia exposure on oxygen consumption, ventilation, diffusive water exchange and ionoregulation in the Pacific hagfish (*Eptatretus stoutii*). Comp Biochem Physiol A Mol Integr Physiol 232:47–59

Giacomin M, Eom J, Schulte PM, Wood CM (2019b) Acute temperature effects on metabolic rate, ventilation, diffusive water exchange, osmoregulation, and acid–base status in the Pacific hagfish (*Eptatretus stoutii*). J Comp Physiol B 189(1):17–35

Greenaway P (1976) The regulation of haemolymph calcium concentration of the crab *Carcinus maenas* (L.). J Exp Biol 64(1):149–157

Harris R, Andrews M (1982) Extracellular fluid volume changes in *Carcinus maenas* during acclimation to low and high environmental salinities. J Exp Biol 99(1):161–173

Healy TM, Schulte PM (2012) Thermal acclimation is not necessary to maintain a wide thermal breadth of aerobic scope in the common killifish (*Fundulus heteroclitus*). Physiol Biochem Zool 85(2):107–119

Henry RP, Garrelts EE, McCarty MM, Towle DW (2002) Differential induction of branchial carbonic anhydrase and Na+/K+ ATPase activity in the euryhaline crab, *Carcinus maenas*, in response to low salinity exposure. J Exp Zool 292(7):595–603

Henry RP, Gehnrich S, Weihrauch D, Towle DW (2003) Salinity-mediated carbonic anhydrase induction in the gills of the euryhaline green crab, *Carcinus maenas*. Comp Biochem Physiol A Mol Integr Physiol 136(2):243–258

Henry RP, Lucu Č, Onken H, Weihrauch D (2012) Multiple functions of the crustacean gill: osmotic/ionic regulation, acid–base balance, ammonia excretion, and bioaccumulation of toxic metals. Front Physiol 3:431

Hill A, Taylor A, Strang R (1991) Physiological and metabolic responses of the shore crab *Carcinus maenas* (L.) during environmental anoxia and subsequent recovery. J Exp Mar Biol Ecol 150(1):31–50

Johnson I, Uglow R (1985) Some effects of aerial exposure on the respiratory physiology and blood chemistry of *Carcinus maenas* (L.) and *Liocarcinus puber* (L.). J Exp Mar Biol Ecol 94(1–3):151–165

Klassen GJ, Locke A (2007) A biological synopsis of the European green crab, *Carcinus maenas*. Can Manusc. Rep Fish Aquat Sci 2818, vii+75pp

Lauff R, Wood C (1996) Respiratory gas exchange, nitrogenous waste excretion, and fuel usage during starvation in juvenile rainbow trout, *Oncorhynchus mykiss*. J Comp Physiol B165(7):542–551

Leignel V, Stillman J, Baringou S, Thabet R, Metais I (2014) Overview on the European green crab *Carcinus* spp. (Portunidae, Decapoda), one of the most famous marine invaders and ecotoxicological models. Environ Sci Pollut Res 21(15):9129–9144

Lucu Č, Siebers D (1986) Amiloride-sensitive sodium flux and potentials in perfused *Carcinus* gill preparations. J Exp Biol 122(1):25–35

McDonald DG, Hõbe H, Wood CM (1980) The influence of calcium on the physiological responses of the rainbow trout, *Salmo gairdneri*, to low environmental pH. J Exp Biol 88(1):109–132

McGaw I, Kaiser MJ, Naylor E, Naylor HRN (1992) Intra-specific morphological variation related to the moult-cycle in colour forms of the shore crab *Carcinus maenas*. J Zool (lond) 228:351–359

McGaw I, Reiber C, Guadagnoli J (1999) Behavioral physiology of four crab species in low salinity. Biol Bull 196(2):163–176

McGaw I (1991). Behavioural responses of the shore crab *Carcinus maenas* to salinity variation. Ph.D. Thesis, University of Wales

McNamara JC, Faria SC (2012) Evolution of osmoregulatory patterns and gill ion transport mechanisms in the decapod Crustacea: a review. J Comp Physiol B 182(8):997–1014

Moore S, Stein WH (1954) A modified ninhydrin reagent for the photometric determination of amino acids and related compounds. J Biol Chem 211:907–913

Morritt D, Spicer JI (1993) A brief re-examination of the function and regulation of extracellular magnesium and its relationship to activity in crustacean arthropods. Comp Biochem Physiol A Mol Integr Physiol 106(1):19–23

Quijada-Rodriguez AR, Allen GJ, Nash MT, Weihrauch D (2022) Postprandial nitrogen and acid-base regulation in the seawater acclimated green crab, *Carcinus maenas*. Comp Biochem Physiol A Mol Integr Physiol 267:111171

Rahmatullah M, Boyde TRC (1980) Improvements in the determination of urea using diacetyl monoxime: methods with and without deproteinisation. Clin Chim Acta 107(1):3–9

Rainbow P, Black W (2001) Effects of changes in salinity on the apparent water permeability of three crab species: *Carcinus maenas*, *Eriocheir sinensis* and *Necora puber*. J Exp Mar Biol Ecol 264(1):1–13

Rasmussen A, Andersen O (1996) Apparent water permeability as a physiological parameter in crustaceans. J Exp Biol 199(12):2555–2564

Rasmussen AD, Bjerregaard P (1995) The effect of salinity and calcium concentration on the apparent water permeability of *Cherax destructor*, *Astacus astacus* and *Carcinus maenas* (Decapoda, Crustacea). Comp Biochem Physiol A Mol Integr Physiol 111(1):171–175

Rudy PP Jr (1967) Water permeability in selected decapod Crustacea. Comp Biochem Physiol 22(2):581–589

Schwabe E (1933) Über die Osmoregulation verschiedener Krebse (Malacostracen). Z Vgl Physiol 19(1):183–236

Shaw J (1961) Studies on ionic regulation in *Carcinus maenas* (L.): I. Sodium balance. J Exp Biol 38(1):135–152

Siebers D, Lucu C, Sperling K-R, Eberlein K (1972) Kinetics of osmoregulation in the crab *Carcinus maenas*. Mar Biol 17(4):291–303

Siebers D, Leweck K, Markus H, Winkler A (1982) Sodium regulation in the shore crab *Carcinus maenas* as related to ambient salinity. Mar Biol 69(1):37–43

Siebers D, Winkler A, Lucu C, Thedens G, Weichart D (1985) Na–K-ATPase generates an active transport potential in the gills of the hyperregulating shore crab *Carcinus maenas*. Mar Biol 87(2):185–192

Siebers D, Lucu Č, Winkler A, Dalla Venezia L, Wille H (1986) Active uptake of sodium in the gills of the hyperregulating shore crab *Carcinus maenas*. Helgol Meeresunters 40(1):151–160

Siebers D, Wille H, Lucu C, Venezia LD (1989) Conductive sodium entry in gill cells of the shore crab, *Carcinus maenas*. Mar Biol 101(1):61–68

Simonik E, Henry RP (2014) Physiological responses to emersion in the intertidal green crab, *Carcinus maenas* (L.). Mar Freshw Behav Physiol 47 (2):101–115

Smith RI (1970) The apparent water-permeability of *Carcinus maenas* (Crustacea, Brachyura, Portunidae) as a function of salinity. Biol Bull 139(2):351–362

Spaargaren D (1982) The ammonium excretion of the shore crab, *Carcinus maenas*, in relation to environmental osmotic conditions. Neth J Sea Res 15(2):273–283

Stewart PA (1978) Independent and dependent variables of acid-base control. Respir Physiol 33(1):9–26

Taylor A (1977) The respiratory responses of *Carcinus maenas* (L.) to changes in environmental salinity. J Exp Mar Biol Ecol 29(2):197–210

Taylor E (1982) Control and co-ordination of ventilation and circulation in crustaceans: responses to hypoxia and exercise. J Exp Biol 100(1):289–319

Taylor E, Butler P, Al-Wassia A (1977) Some responses of the shore crab, *Carcinus maenas* (L.) to progressive hypoxia at different acclimation temperatures and salinities. J Comp Physiol 122(3):391–402

Truchot J (1973) Fixation et transport de l'oxygène par le sang de *Carcinus maenas*: variations en rapport avec diverses conditions de température et de salinité. Neth J Sea Res 7:482–495

Truchot J (1975) Factors controlling the in vitro and in vivo oxygen affinity of the hemocyanin in the crab *Carcinus maenas* (L.). Respir Physiol 24(2):173–189

Truchot JP (1976a) Carbon dioxide combining properties of the blood of the shore crab *Carcinus maenas* (L): carbon dioxide solubility coefficient and carbonic acid dissociation constants. J Exp Biol 64(1):45

Truchot JP (1976b) Carbon dioxide combining properties of the blood of the shore crab, *Carcinus maenas* (L.): CO_2-dissociation curves and Haldane effect. J Comp Physiol 112(3):283–293

Truchot J, Forgue J (1998) Effect of water alkalinity on gill CO_2 exchange and internal PCO_2 in aquatic animals. Comp Biochem Physiol A Mol Integr Physiol 119(1):131–136

Truchot J-P (1981) The effect of water salinity and acid-base state on the blood acid–base balance in the euryhaline crab, *Carcinus maenas* (L.). Comp Biochem Physiol A Mol Integr Physiol 68(4):555–561

Truchot J-P (1987) Comparative aspects of extracellular acid-base balance, zoophysiology, vol 20. Springer, Berlin

Verdouw H, Van Echteld CJA, Dekkers EMJ (1978) Ammonia determination based on indophenol formation with sodium salicylate. Water Res 12(6):399–402

Wang S, Carter CG, Fitzgibbon QP, Smith GG (2021) Respiratory quotient and the stoichiometric approach to investigating metabolic energy substrate use in aquatic ectotherms. Rev Aquac 13(3):1255–1284

Webb D (1940) Ionic regulation in *Carcinus maenas*. Proc R Soc Lond Ser B Biol Sci 129(854):107–136

Weihrauch D, Becker W, Postel U, Luck-Kopp S, Siebers D (1999) Potential of active excretion of ammonia in three different haline species of crabs. J Comp Physiol B 169(1):25–37

Weihrauch D, Fehsenfeld S, Quijada-Rodriguez A (2017) Nitrogen excretion in aquatic crustaceans. Acid–base balance and nitrogen excretion in invertebrates: In: Weihrauch D, O'Donnell MJ (eds) Acid–base balance and nitrogen excretion in invertebrates, pp 1–24. Springer, Cham

Wilson CH, Nancollas SJ, Rivers ML, Spicer JI, McGaw IJ (2021) Effects of handling during experimental procedures on stress indices in the green shore crab, *Carcinus maenas* (L.). Mar Freshw Behav Physiol 54(2):65–86

Winkler A (1986) The role of the transbranchial potential difference in hyperosmotic regulation of the shore crab *Carcinus maenas*. Helgol Meeresunters 40(1):161–175

Zanders I (1980) Regulation of blood ions in *Carcinus maenas* (L.). Comp Biochem Physiol A Mol Integr Physiol 65(1):97–108

Zatta P (1987) The relationship between plasma proteins and intracellular free amino acids during osmotic regulation in *Carcinus maenas*. J Exp Zool 242(2):131–136

Zimmer AM, Wood CM (2017) Acute exposure to high environmental ammonia (HEA) triggers the emersion response in the green shore crab. Comp Biochem Physiol A Mol Integr Physiol 204:65–75